Available online at www.sciencedirect.com
SCIENCE DIRECT
Biochimica et Biophysica Acta 1715 (2005) 132 – 144
BIOCHIMICA ET BIOPHYSICA ACTA
BBA
http://www.elsevier.com/locate/bba

Characterization of CLCA protein expressed in ductal cells of rat salivary glands

Jun Yamazaki [a,*], Kazuhiko Okamura [b], Kazunari Ishibashi [c], Kenji Kitamura [a]

[a] Department of Physiological Science and Molecular Biology, Fukuoka Dental College, 2-15-1 Tamura, Sawara-ku, Fukuoka 814-0193, Japan
[b] Department of Morphological Biology, Fukuoka Dental College, Sawara-ku, Fukuoka 814-0193, Japan
[c] Department of Functional Bioscience, Fukuoka Dental College, Sawara-ku, Fukuoka 814-0193, Japan

Received 24 June 2005; received in revised form 4 August 2005; accepted 4 August 2005
Avilable online 19 August 2005

Abstract

A molecular entity for Ca^{2+}-dependent Cl^- transport has not been well characterized in salivary cells. Here, we identify a rat CLCA homologue (rCLCA1) using a polymerase chain reaction (PCR)-based strategy. The full length of the isoform was 3.3 kb, and the predicted open reading frame encoded a 903-amino acid protein. Immunoblotting using a specific anti-rCLCA antibody recognizing near the amino-terminus showed the expression of N-glycosylated 120- and 86-kDa proteins in the membrane fraction of rCLCA1-transfected HEK293 cells. Reverse transcription-PCR results showed mRNA expressions in rat submandibular gland (SMG), ileum, and lung. Intense immunostaining was detected in the striated ducts, but not in the acinar cells, of SMG. Immunoblot for the membrane fraction of SMG revealed the existence of 137- and 90-kDa protein species. N-glycosidase F reduced the size of these bands toward those of the deglycosylated forms in the transfected HEK293 cells. A marked ionomycin-induced Cl^- conductance was observed in the transfected cells. The current was Ca^{2+}-dependent and sensitive to niflumic acid and DIDS. rCLCA1 proteins are probably responsible for modulation of Ca^{2+}-dependent Cl^- transport in salivary ductal cells, where the 137- and 90-kDa proteins may be modified posttranslationally in a manner similar to those in the heterologous expression system.

Keywords: Ca^{2+}-activated Cl^- channel; CLCA; N-glycosylation; Epithelium; Submandibular gland; Ileum

1. Introduction

Ca^{2+}-activated Cl^- channels are found in a variety of tissues, including epithelium, cardiac and smooth muscle, and neurons [1,2]. These channels play an important role in cell excitability and muscle tonus, as we have already reported in canine atrial myocytes and rat cerebral arteriolar smooth muscle cells [3,4]. In epithelial cells, Ca^{2+}-activated Cl^- channels are involved in anion transport and fluid secretion, and in cystic fibrosis patients they may effectively substitute non-functional cystic fibrosis transmembrane regulator (CFTR) Cl^- channels [5].

Multiple classes of Cl^- channels (including CFTR, CLC, and Ca^{2+}-activated Cl^- channels) have been described in salivary acinar and ductal cells [6]. In electrophysiological studies, the Ca^{2+}-activated Cl^- channels present on salivary acinar and ductal cells have been found to show time-dependent behaviour, and also sensitivity to both 4,4′-diisothiocyanato-stilbene-2,2′-disulfonic acid (DIDS) and niflumic acid [2]. The physiological relevance of Ca^{2+}-activated Cl^- channels in acinar cells has been described as follows [6]; increase in the intracellular Ca^{2+} concentration triggers Cl^- efflux through the luminal membrane. Such transepithelial Cl^- movement and paracellular Na^+ transport into the lumen play a key role in establishing the osmotic driving force for water movement. The channels and transporters present in ducts are less well understood, although apical Na^+ and Cl^- channels are assumed to provide an effective influx mechanism for NaCl reabsorp-

* Corresponding author. Tel.: +81 92 801 0411x669; fax: +81 92 801 4909.
E-mail address: junyama@college.fdcnet.ac.jp (J. Yamazaki).

0005-2736/$ - see front matter © 2005 Elsevier B.V. All rights reserved.
doi:10.1016/j.bbamem.2005.08.001

tion [6]. Despite their possible pivotal contribution to the production of the final saliva, a molecular entity for these ductal ion channels has not been well characterized.

The first reported clone of candidates for Ca^{2+}-activated Cl^- channels or for modulators of these channels, from bovine tracheal epithelium, was bCLCA1 [7], which had formerly been isolated as an anion-conducting protein using a biochemical technique. This prototype was followed by cloning of other members of the CLCA family: viz. another bovine isoform, from lung endothelial cells, that had been identified as an adhesion molecule (Lu-ECAM-1 or bCLCA2) [8], four from human tissues (hCLCA1–4) [9–11], six from murine tissues (mCLCA1–6) [12–15], and one from porcine ileum (pCLCA1) [16]. The sequence similarities among these members indicate that posttranslational processing produces an N-glycosylated heterodimer with a 90-kDa amino-terminal subunit possessing conserved spacing of cysteine residues and a 30- to 40-kDa carboxyl-terminal subunit, either or both of which are predicted to anchor to the plasma membrane [10,11]. Although CLCAs, and the more recently identified channel bestrophin, have been documented in various types of tissues [2,17,18], none of these proteins has been shown to be expressed in salivary ductal cells.

We employed a reverse-transcription (RT)-PCR-based strategy to identify the CLCA member present in rat tissue, using total RNA extracted from the ileum, with the aid of primers based on the cDNA sequence conserved among mCLCA1, 2, and 4. We cloned the rat homologue (rCLCA1) of a CLCA family member, and then confirmed an expression of a Ca^{2+}-activated Cl^- conductance in human embryonic kidney 293 (HEK293) cells transfected with this homologue. This isoform is the first CLCA protein shown to be expressed in the striated ductal cells of the rat submandibular gland (SMG). In that gland, rCLCA1 protein is likely to be responsible for modulation of Ca^{2+}-dependent transport of Cl^-. Additionally, the present biochemical results obtained using a specific antibody suggest that the existence of different immunoreactive protein species is due to posttranslational processing of rCLCA1, including N-glycosylation and monobasic proteolysis.

2. Materials and methods

2.1. Identification of CLCA from rat ileum

Male Wistar rats (6 weeks old) were anesthetised with sodium pentobarbital, permission for the procedures used having been granted by the Animal Research Committee of Fukuoka Dental College. Total RNA was prepared from the ileum, left ventricle, and aorta by grinding the tissue with a pestle and subsequent extraction with Isogen (Nippongene, Japan). RNA (1 μg) was reverse-transcribed at 42 °C using 10 units/μl of Superscript II RNase H^- reverse transcriptase (Invitrogen Corp., CA, USA) and oligo(dT) primer. The cDNA was subjected to PCR for 40 cycles under a low-stringency condition (denaturation, 94 °C, 30 s; annealing, 59 °C, 1 min; extension, 72 °C, 2 min) using 0.025 unit/μl of Taq polymerase (Takara LA Taq; Takara Bio Inc., Japan) together with primers based on the cDNA sequence conserved among mCLCA 1, 2, and 4 [12,14,15]. The forward primer was 5′-CATTGCCATTAACCCCAGTG-3′ and the reverse primer 5′-GCCTCCAGGTCTGTGACTTTAC-3′ (T_m=63–65 °C; the underlined nucleotides showing discrepancy with the rCLCA1 cDNA sequence as finally determined). The PCR product was obtained only from ileum, with a length of 2.1 kb (as predicted from the cDNA sequences of mCLCA members). The ileal product (nt 125–2323 of rCLCA1) was gel-purified and cloned into 3′-deoxythymidine overhangs of a pCR-XL-TOPO vector (Invitrogen Corp.). After transformation of competent cells, six positive clones were picked up, and the DNA insert was sequenced. Automated sequencing was performed using BigDye Terminator cycle sequencing on an ABI Prism 377 DNA sequencer (PE Applied Biosystems, USA). These six clones were almost identical, there being only a 0.2% nucleotide divergence, and this may have been due in part to a PCR amplification error. The determined rCLCA1 cDNA sequence possessed 87% homology to mCLCA 1 and 2, and 84% to mCLCA4.

2.2. Construction of full-length rat CLCA cDNA

Using oligo-dT-primed ileal cDNA, a gene-specific primer (nt 2242–2259; 5′-AGTCGTTTACTGTGTCCG-3′) and a primer recognizing the oligo(dT) adaptor sequence were employed for 3′ rapid amplification of cDNA ends (3′-RACE) (RNA LA PCR Kit; Takara Bio Inc.). The specificity of the 3′-RACE product was confirmed when a smaller-sized band was found to be obtained in the second PCR reaction with the nested primer (nt 2302–2321; 5′-GTAAAGTTA-CAGACCTGGAG-3′). 5′-RACE was performed to clone the 5′-end of rCLCA1 cDNA (5′-Full RACE Core Kit; Takara Bio Inc.). A 5′-phosphorylated gene-specific primer (nt 698–712; 5′-TGAATTTTGTCTGGG-3′) was used to reverse-transcribe the cDNA obtained from rCLCA1 mRNA. After the formation of concatenate or circular cDNA with T4 DNA ligase, gene-specific primers, and thereafter the nested primers, were used to perform two-step amplification of the 5′-end of the cDNA. The PCR products were cloned to a pCR-XL-TOPO vector, and sequenced. The 176-bp 5′-RACE product contained an ATG codon conforming a Kozak translation initiation sequence, together with a signal sequence similar to that of the mCLCA members. The 1068-bp 3′-RACE product contained the TAG stop codon followed by a 577-bp untranslated region and a poly(A^+) tail. The three PCR products obtained above (nt 1–176, 125–2323, and 2242–3309 of rCLCA1) were well overlapped (AutoAssembler; PE Applied Biosystems).

To confirm the existence of the contiguous cDNA comprising these PCR products, we designed a forward primer corresponding to a region encompassing a Kozak sequence and ATG codon (nt 16–31, 5′-CGAGCATGG-

TGCCAGT-3′) and a reverse primer corresponding to a region initiating at 91 bp downstream of the stop codon (nt 2803–2823, 5′-GTTGACAGGCAGACATTGAGT-3′). The entire open reading frame (ORF) for rCLCA1 along with part of its 5′- and 3′-untranslated regions was amplified, with oligo(dT)-primed ileal cDNA serving as a template, using 0.05 unit/μl of PfuUltra High-fidelity DNA polymerase (Stratagene, La Jolla, CA, USA). The PCR condition consisted of initial denaturation for 2 min at 95 °C (hot start), then 35 cycles of denaturation (95 °C, 30 s), annealing (56 °C, 30 s), and extension (72 °C, 3 min), plus a final extension step (72 °C, 10 min). A deoxyadenosine was added to the 3′-end of the PCR product through the terminal deoxynucleotidyl transferase activity of Taq polymerase (Takara Bio Inc.), and it was then cloned into a pCR-XL-TOPO vector. The insert was sequenced using BigDye Terminator cycle sequencing, and was found to be well matched to the sequence produced by a combination of the three overlapping PCR products described above. The plasmid was cleaved with *Bam*H I and *Not*I, and the fragment was subcloned into the corresponding site in the expression vector. The nucleotide sequence of rCLCA1 has been submitted to the GenBank/EMBL Data Bank with the accession number AB119249.

2.3. Organ Distribution of rCLCA1 by RT-PCR

Rat and mouse tissues were dissected, and total RNA was extracted using Isogen (Nippongene). Total RNA (2 μg) was reverse-transcribed as described before using random 9-mers. The cDNA was subjected to PCR for 40 cycles under a high-stringency condition (denaturation, 94 °C, 30 s; annealing, 56 °C, 30 s; extension, 72 °C, 1 min) using 0.025 unit/ml of Taq polymerase (Takara Bio Inc.). Primer pairs specific for rCLCA1 were designed to recognize cDNA sequence 970–1424 (forward, 5′-GAAGCATGGACA-GAAG-3′; reverse, 5′-GCTGTTCACATCTTTGTTG-3′). No PCR amplification was observed when the total RNA preparation was used without treatment with reverse transcriptase (-RT), arguing against genomic DNA contamination. The primers seemed to bracket three introns, according to the intron–exon boundaries reported for the hCLCA1 gene, and would have been able to demonstrate the existence of any 5.7-kb DNA fragment in the event of genomic DNA contamination. DNA amplification, however, was not detected at a longer size than that presumed to be derived from mRNA (455 bp). The selectivity of the primer was confirmed in control experiments on mouse ileum and lung, which are reported to contain mCLCA4 and mCLCA1 and 4, respectively [12,14]. As a housekeeping control, specific primers were also used for amplification of the cDNA transcribed from glyceraldehyde-3-phosphate dehydrogenase (GAPDH) mRNA (nt 1457–1476 and nt 1617–1636; GenBank accession number AF106860). PCR products were analysed on an ethidium bromide-stained agarose (2%) gel.

2.4. Fractionation procedure

Proteins were prepared either from lysates of rCLCA-transfected HEK293 cells or from lysates of rat salivary gland, ileum, and lung dissected from 6- to 8-week-old Wistar rats. To prepare the cytosolic fraction, HEK293 cells were homogenised in lysis buffer A (150 mM NaCl, 1 mM EDTA, and 20 mM HEPES, pH=7.5) in the presence of protease inhibitors (2 mM phenylmethylsulfonyl fluoride, 10 μM leupeptin, 1.5 μM pepstatin A, 40 μM bestatin, and 10 μg/ml aprotinin) using a sonicator, followed by centrifugation at 100 kG for 1 h, and the supernatant was then collected. The rat tissues mentioned above were homogenised in lysis buffer B [250 mM sucrose, 1 mM EGTA, 1 mM dithiothreitol (DTT) and 10 mM PIPES, pH=6.8] in the presence of the above protease inhibitors plus 100 μg/ml trypsin inhibitor using a Teflon homogenizer. Then, the homogenate was centrifuged at 1 kG for 10 min. The supernatant (1 kG Sup) was centrifuged consecutively at 6 kG for 15 min and at 200 kG for 3 h. The supernatant obtained in the final step above was collected for the cytosolic fraction. For the membrane fractions from HEK293 cells and the various rat tissues, the pellet obtained after the centrifugation in the final step was treated for 30 min with 1% TritonX-100-containing lysis buffer A or B, respectively, followed by centrifugation at 100 kG for 1 h, and the supernatant was used. All procedures described above were performed at 4 °C. The protein concentration was measured using bicinchoninic acid (BCA Protein Assay Kit; Pierce, IL, USA).

2.5. Immunoblotting analysis

An anti-rCLCA polyclonal antibody was generated against a synthetic peptide based on the region of the N-terminal external domain (SKSEYLMPKRESYDKAD). The peptide was conjugated to keyhole limpet hemocyanin, and then used to immunize a rabbit. Immune serum was affinity-purified using the peptide coupled to CNBr-activated Sepharose (Amersham Pharmacia Biotech). Protein samples were boiled in the presence of 2% SDS and 10 mM DTT, unless otherwise stated, then subjected to SDS-PAGE (7.5%), and finally blotted to PVDF membrane (Hybond-P; Amersham). Immunoblots were obtained using the anti-rCLCA antibody (dilution; 1:8000) followed by horseradish peroxidase (HRP)-conjugated anti-rabbit immunoglobulin G (IgG) antibody (dilution, 1:400,000; Jackson ImmunoResearch Lab. Inc.), and detected by means of enhanced chemiluminescence (ECL Advance; Amersham).

For biotinylation, rCLCA-transfected HEK293 cells were treated with biotinamidocaproate N-hydroxysuccinamide ester (ECL Protein Biotinylation Module, Amersham) as recommended by the manufacturer. The cells were lysed in the presence of 1% Triton-X 100, and the proteins were immunoprecipitated using the anti-rCLCA antibody bound to rProtein A Sepharose (Amersham), then analysed by SDS-PAGE, blotted to PVDF, and finally detected using strepta-

vidine–HRP conjugate and enhanced chemiluminescence. For glycosidase digestion, the membrane fraction was denatured by boiling in 0.2% SDS for 10 min. Triton X-100 was added (final volume, 1.5%) prior to incubation with N-glycosidase F (PNGase F, Sigma) in Na phosphate buffer (pH = 7.5) at 37 °C for 18 h. The reaction product was denatured by boiling for 5 min, then used for SDS-PAGE and immunoblotting.

2.6. Immunostaining

HEK293 cells in a tissue-culture plate were washed with Ca^{2+}- and Mg^{2+}-free phosphate buffer (PBS), then fixed with 2% paraformaldehyde in PBS. The cells, which were not permeabilized, were immersed in 1.5% goat serum, then incubated in PBS containing rabbit anti-rCLCA antibody (dilution, 1:400). Next, they were washed and incubated with goat anti-rabbit IgG conjugated with biotin. Finally, they were washed and reacted for 10 min with an avidin–biotinylated HRP complex (Vectastain ABC kit; Vector Lab., Burlingame, USA). Immunostaining was visualized using 3,3′-diaminobenzidine (DAB) in imidazole buffer containing H_2O_2 (Envision+kit/HRP; Dako Co., Carpinteria, USA).

Formalin-fixed 5-μm-thick tissue sections were mounted on slides coated with silane (3-aminopropyltriethoxy-silane; Sigma Chemical Co., MO, USA), then immersed with 0.3% H_2O_2 in absolute methanol for 20 min to block endogenous peroxidase activity, washed in PBS, and finally incubated in 10% normal rabbit serum to block any non-specific binding of the antibody. The sections were then incubated with polyclonal rabbit anti-rCLCA antibody (diluted 1:300) for 3 h at room temperature. The bound antibody was detected by the Universal Immuno-enzyme Polymer (UIP) method (Histofine Simple Stain Rat MAX PO kit; Nichirei Co., Tokyo, Japan). After the reaction of amino acid polymers conjugated to multiple molecules of the secondary antibody with peroxidase, the sections were treated with 0.02% DAB tetrahydrochloride (Dojin Laboratories, Kumamoto, Japan) in PBS together with 0.003% H_2O_2, then counterstained with 1% methylgreen.

Throughout the cellular and tissue immunostaining procedures, confirmation of the specificity of the immunoreaction was performed by incubating samples with non-immunized rabbit serum or PBS instead of the primary antibody. No immunoreaction was found in such preparations.

2.7. Subcloning into expression vector and whole-cell patch recording

For the expression study, rCLCA1 cDNA was subcloned into mammalian expression vector pIRES-hrGFP-1a (Stratagene). This construct contains a dicistronic expression cassette in which part of the 5′- and 3′-untranslated regions flanking the coding region of rCLCA1 cDNA is followed by an internal ribosomal entry site linked to the humanized recombinant GFP (hrGFP) coding sequence.

HEK293 cells were transfected either with the rCLCA1-expressing pIRES-hrGFP-1a vector or with vector alone (FuGENE 6; Roche Molecular Biochemicals, IN, USA). The cells were dissociated 24 h later with the aid of 0.025% EDTA-containing Ca^{2+}, Mg^{2+}-free PBS, then seeded on poly-L-lysine-coated coverslips. After 12 h, each coverslip was placed in a chamber on the stage of an inverted microscope (Diaphot-300; Nikon, Tokyo, Japan) and superfused with bath solution at 1.5–2.0 ml min^{-1}. The standard bath solution contained (in mM): NaCl 140, CsCl 5, $CaCl_2$ 1.8, $MgCl_2$ 1.2, D-glucose 11, HEPES 10, mannitol 20–30 (pH = 7.4; 320–330 mosM kg^{-1} H_2O). The pipette solution for whole-cell recording contained (in mM): CsCl 145, $CaCl_2$ 0.366, $MgCl_2$ 2.2, glycol-bis(β-aminoethylether)-*N*,*N*,*N*′,*N*′-tetraacetic acid 1, ATP-Mg 1, HEPES 10, mannitol 10 (pH = 7.2; 310 mosM kg^{-1} H_2O). Free intracellular [Ca^{2+}] was estimated to be 63 nM, according to a utility software for the calculation of free cation concentrations (Calcon for Windows).

The patch pipettes had a tip resistance of 1.5 to 2.5 MΩ. Ag/AgCl wires immersed in the bath and pipette solutions were connected to a patch-clamp amplifier (Axopatch 200A; Axon Instruments, Foster City, CA, USA). Changes in junctional potentials created between the pipette and the bath solutions were corrected. An ultraviolet light was used to select hrGFP-positive cells for current recording. After giga-ohm seal-formation, the cells were voltage-clamped at −50 mV. The current–voltage (*I*–*V*) relationship was obtained by measuring the current amplitude (averaged from 70 ms to the end of the pulse) evoked by each 300- ms voltage step within the range −80 to 80 mV from a holding potential of −50 mV. Experiments were performed at room temperature. The currents were filtered at a frequency of 1 kHz, digitised on-line at 5 kHz using an IBM-compatible computer, and analysed using pCLAMP 8.0 software (Axon Instruments, CA, USA).

Data are expressed as means ± SEM (n, number of observations). Statistical analysis was performed using a paired or unpaired t-test (SigmaPlot 2000; SPSS Inc., IL, USA). A *P* value less than 0.05 was considered to be statistically significant. Ionomycin, DIDS, and niflumic acid (Sigma) were freshly dissolved as stock solutions in dimethylsulfoxide (DMSO). The final concentration of DMSO (less than 0.1%) did not by itself affect currents when applied externally. Other compounds were dissolved as stock solutions in deionized water.

3. Results

3.1. Molecular cloning of rCLCA1

To identify the CLCA member present in rat tissue, total RNA samples extracted from rat ileum, aorta, and left

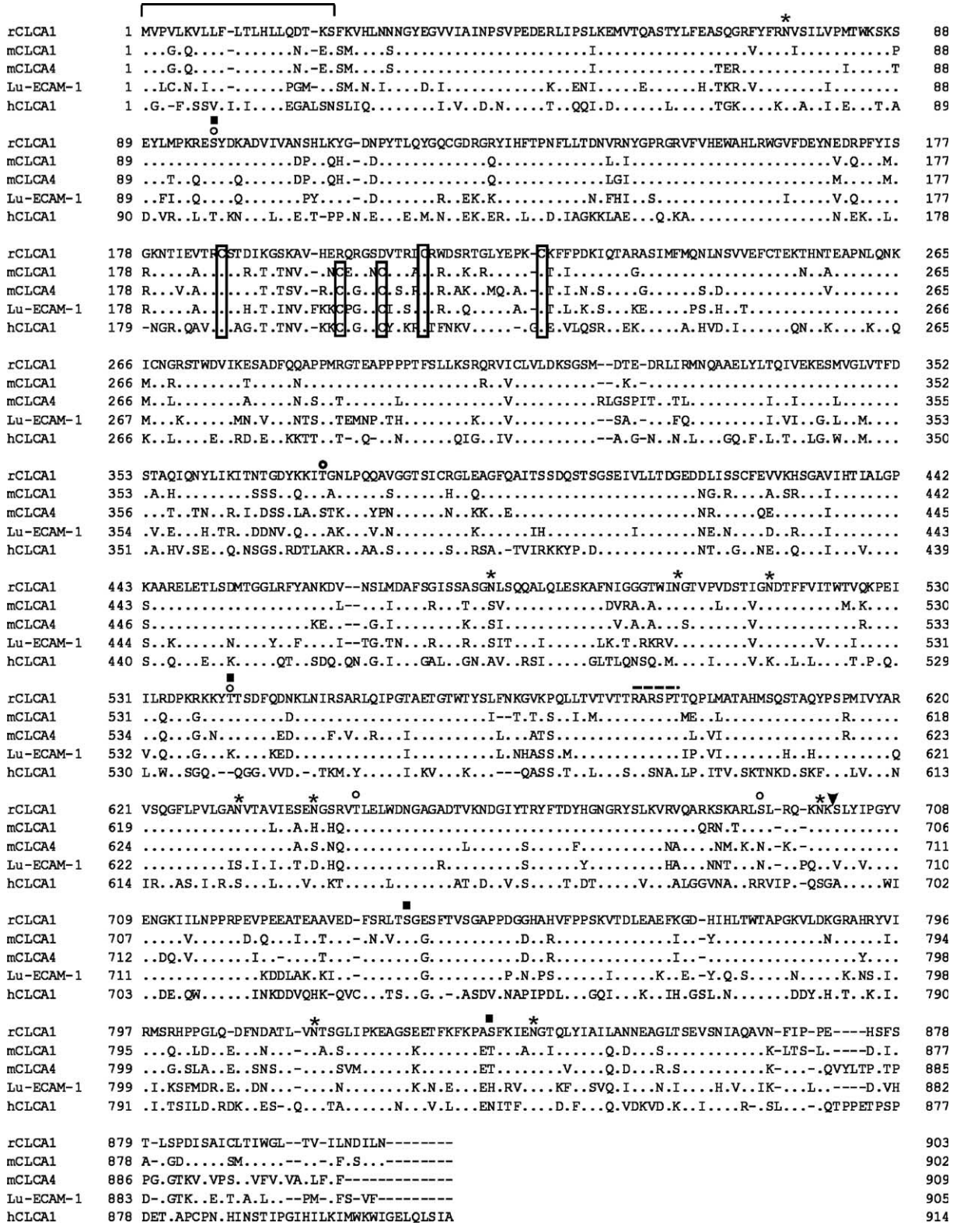

Fig. 1. Alignment of amino acid sequences of rCLCA1, mCLCA1, mCLCA4, Lu-ECAM-1, and hCLCA1. Dots indicate amino acid residues identical to those in rCLCA1, while dashes indicate missing residues. Potential N-glycosylation sites are shown by asterisks, and the signal sequence by the overline bracket. The proposed processing site is indicated by an arrowhead. Conserved cysteine residues are indicated by boxes. Predicted sites for phosphorylation by PKA and CaMKII are indicated by open circles and closed squares, respectively (Motif Scan program). Adjacent sites for phosphorylation by several kinases are shown by the broken line [12]. Multiple alignment (Clustal method) was performed using Genetyx-Mac ver. 12 from Genetyx Corp, Japan. GenBank accession numbers are AB119249 (rCLCA1), AF047838 (mCLCA1), AY008277 (mCLCA4), AF001261 (Lu-ECAM-1), and AF039400 (hCLCA1).

ventricle were subjected to RT-PCR. The primers designed for PCR were based on the cDNA sequence that is identical among mCLCA1, 2, and 4. Only the rat ileal preparation exhibited a PCR product with a size of approximately 2.1 kb. This length is consistent with that of the primers-flanking nucleotide sequences for mCLCA1, 2, and 4. Sequencing of the PCR product revealed 87, 87, and 84% nucleotide homology to mCLCA1, 2, and 4 mRNA, respectively, suggesting that the cDNA represents a rat CLCA homologue. By assembling this sequence with sequences obtained using 5′- and 3′-RACE, the full length of the new CLCA isoform (rCLCA1) was determined. The sequence consists of 3309 bases, of which 20 bases comprise the 5′-untranslated region and 580 bases the 3′-untranslated region followed by a poly(A)$^+$ tail. The poly(A)$^+$ tail is preceded by a polyadenylation signal (AATAAA), the separation between the two being 12 bp. The ORF was predicted to encode a 903-amino acid protein (Fig. 1).

To confirm the existence of the contiguous cDNA predicted from the assembled sequences, two specific primers based on the assembled sequences were designed to correspond to a region encompassing a Kozak sequence and a region downstream of the stop codon. The sequence of the PCR product obtained using PfuUltra DNA polymerase with high fidelity was well matched to the sequence produced by a combination of the three overlapping PCR products (nt 16–2823).

A rat genomic sequence has been reported recently [19]. We performed a BLAST search using rCLCA1 cDNA as the query sequence [20]. The regions were found to be identical to a predicted mRNA sequence XM_575054, derived from the contig NW_047633 residing in chromosome 2, except for a mismatching 4 bp for the coding region, resulting in alteration of two amino acids at 845 (L for I) and 860 (E for K). The locus of the rCLCA1 gene appears to be 2q44. On the basis of the above comparison, the gene was predicted to consist of at least 14 exons interspersed with 13 introns, and to span 22,293 bp from the start to the end of the cDNA. The genome sequence was scanned from 5,500 bp upstream of the start to 979 bp downstream of the corresponding cDNA sequence using GENSCANW software (available on World Wide Web). The software predicted 14 exons and 13 introns with the same intron–exon boundaries as those obtained from the comparison between genome and cDNA sequences, except for the estimation of the fourth and eleventh exons due to the prediction by the software of 5′- and 3′-splice sites with lower probability scores.

The predicted full rCLCA1 amino acid sequence was 83% identical to those of mCLCA1 and mCLCA2, and 77% to that of mCLCA4 (Fig. 1). The homologies of the rCLCA1 amino acid sequence to Lu-ECAM-1 and hCLCA1 were lower (70% and 52%, respectively). A phylogenetic tree constructed from the predicted amino acid sequences of murine, bovine, human, and porcine CLCA members indicated that rCLCA1 is most closely related to mCLCA1 and 2, and has a weaker relationship with the hCLCA2 isoform (Fig. 2). A partial sequence of a 110-bp cDNA from the rat was previously entered in the GenBank/EMBL database (accession number AF077303). This partial cDNA sequence, which has not been characterized further, correlated with the sequence (nt 2466–2575) near the 3′-end of rCLCA1 ORF, except for a mutation of A for C (nt 2553). No significant homology to any other proteins was detected using the BLAST algorithm [20]. A homology search of the rat expressed sequence tag (EST) database (537,000 sequences) was performed, and four EST clones from rat cornea were found with lengths of 361 to 532 bases and an identity >97% with respect to partial sequences of rCLCA1 (GenBank accession numbers: CB614498, CB615578, CB615983, and CB801016).

As shown in Fig. 2, hydropathy analysis based on the Kyte–Doolittle index revealed that fully hydrophobic successive regions are located at the amino-terminus and the carboxyl-terminus, as well as in several minor regions present in the intermediate part of the sequence. The cleavable signal sequence in the hydrophobic amino-terminal region indicates the extracellular location of the amino-terminus of this protein (overline bracket in Fig. 1).

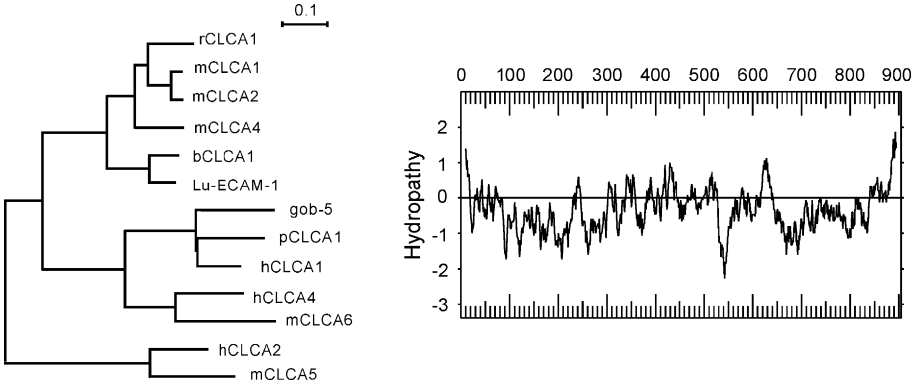

Fig. 2. Phylogenetic tree for CLCA channels (left) and hydropathy plot for rCLCA1 amino acid sequence (right). The tree was constructed (Neighbour-Joining method) from a multiple alignment (Clustal method) of the predicted amino acid sequences for rCLCA1 and the eight related CLCA members (ClustalW ver. 1.81 and Njplot, available on the World Wide Web). Scale bar indicates 10% divergence. Hydropathy plot was constructed using the Kyte–Doolittle algorithm (window size, 19 amino acids). Horizontal numbers denote number of amino acid residues. The plot was made using DNA Strider ver. 1.2.

Another highly hydrophobic region (20 amino acids) located in a sequence near the carboxyl-terminus is likely to be a membrane-spanning domain. Among other CLCA members, transmembrane topology seems still to be controversial [10,11]. According to our predictions of transmembrane helices made using programs PSORT II and SOSUI (available on the World Wide Web), only one transmembrane domain is predicted by these two programs (amino acids 880–902 or 886–902, respectively) to exist in the carboxyl-terminus of rCLCA1. This corresponds to the location of the highest value for the Kyte–Doolittle index, in the extreme carboxyl-terminal part (Fig. 2).

Motif analysis revealed that the predicted protein contains a monobasic proteolytic cleavage site at residue S701 that is conserved among mCLCA1, 2, and 4 (Fig. 1), suggesting the rCLCA1 precursor is cleaved into two components post-translationally. A typical feature of the predicted amino acid sequence is that the rCLCA1 protein contains a lower conserved spacing of cysteine residues than the other CLCA members [i.e., two cysteine residues are replaced by arginine and aspartic acid at residues 200 and 205 (Fig. 1)]. The rCLCA1 sequence contains nine potential sites for N-linked glycosylation. There are several phosphorylation sites for protein kinase A (PKA) and Ca^{2+}/calmodulin kinase II (CaMK II) in CLCA members [7,10,16]. Two adjacent sites for phosphorylation by several kinases (RARSPT; residues 589–594 of rCLCA1) are preserved among rCLCA1, mCLCA1, 2, and 4, and Lu-ECAM-1 [12].

3.2. Tissue expression of rCLCA1 mRNA

To test whether the pair of designed primers recognize rCLCA1 mRNA, we transfected the rCLCA1 cDNA expression vector or the mock vector transiently into HEK293 cells, then performed RT-PCR using total RNA extracted from these cells. Expression of rCLCA1 mRNA at the predicted nucleotide size of 455 bp was strongly detected in rCLCA1-transfected HEK293 cells, but not in mock (hrGFP alone)-transfected or non-transfected cells (Fig. 3A). Using these primers, expressions of rCLCA1 mRNA were not observed in mouse ileum or lung (Fig. 3B), where mCLCA1 and mCLCA4 mRNAs were shown to be expressed abundantly [12,14]. Thus, these primers seemed to be able to discriminate the mRNA for rCLCA1 from those for other CLCA members. Several types of tissue were dissected from rat, and RT-PCR was performed using these primers. A PCR product dependent on RT with a nucleotide size of 455 bp was found be strongly expressed in ileum and SMG (Fig. 3B, C and D). Expression was also significant in stomach, lung, liver, and spleen, and in the sublingual (SLG) and parotid (PG) glands, but no expression was detected in left ventricle or aorta (Fig. 3C and D).

3.3. Heterologous expression of glycosylated rCLCA1 protein in HEK293 cells

First, we examined the subcellular distribution of rCLCA1 protein in a Western blot study using an anti-rCLCA antibody raised against a synthetic peptide corresponding to the amino-terminus of rCLCA (Fig. 4A). The antibody recognized 86-kDa-sized bands strongly in both total cell lysates and the membrane fraction, but far less strongly in the cytosolic fraction of the transfected HEK293 cells, under disulfide-reducing conditions. A faint 120 kDa band was also detected in both total lysate and membrane fractions, but not in the cytosolic fraction.

Next, we examined the expression of the rCLCA on the plasma membrane using surface biotinylation of the rCLCA-transfected HEK293 cells. Plasma membrane proteins were surface-biotinylated before the cells were lysed. The streptavidin–HRP staining of the blot of the lane loaded with total lysate was dense, suggesting an abundant presence of surface proteins (Fig. 4B). Western blotting using anti-rCLCA antibody showed that an 86-kDa protein

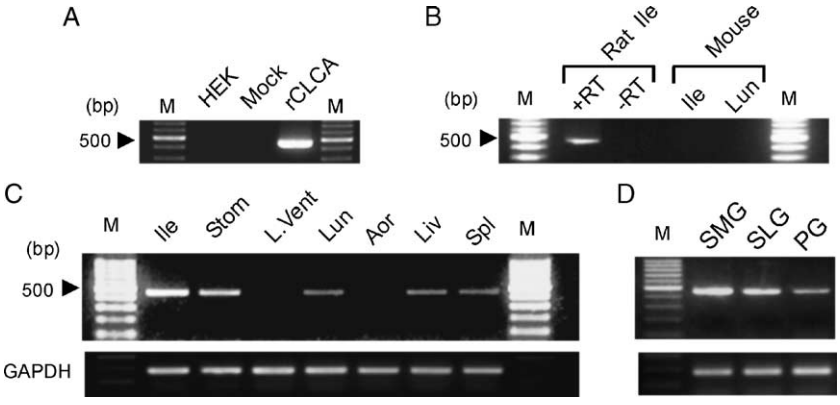

Fig. 3. Expression of rCLCA1 mRNA as determined by RT-PCR. (A, B), expression of PCR product was examined in non-transfected HEK293 cells (HEK) and in HEK293 cells transfected either with the rCLCA1-inserted pIRES-hrGFP-1a vector (rCLCA1) or with the vector alone (Mock) (A) and in rat and mouse tissues (Ile and Lun) (B). +RT, reverse-transcribed preparation. −RT, non-reverse-transcribed preparation. (C, D), tissue distribution was examined in whole rat organs: ileum (Ile), stomach (Stom), left ventricle (L. Vent), lung (Lun), aorta (Aor), liver (Liv), spleen (Spl), submandibular gland (SMG), sublingual gland (SLG) and parotid gland (PG). GAPDH mRNA was also amplified, as an internal control for the amount of mRNA (180-bp bands).

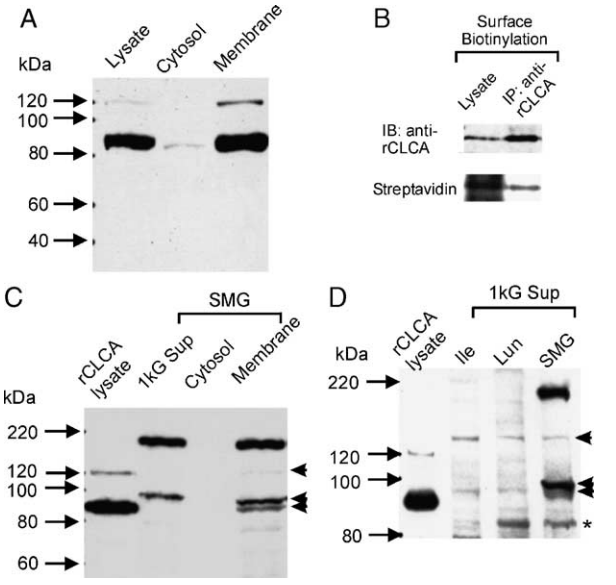

Fig. 4. Western blotting analyses of proteins fractionated from rCLCA-transfected HEK293 cells (A) and from rat submandibular gland (SMG), ileum (Ile), and Lung (Lun) (C, D). Fractionation and immunodetection were performed as described in Materials and methods. In B, the transfected HEK293 cells were surface-biotinylated. The biotinylated protein from the cell lysate and its immunoprecipitate (using anti-rCLCA antibody) were detected by streptavidin–HRP. Samples were boiled for 5 min under reducing condition (10 mM DTT). Protein loading was: 10 μg per lane in A; 20 μg per lane in B lysate; 2.5 μg per rCLCA lane and 25 μg per each other lane in C; 2.5 μg per rCLCA lane and 50 μg per each other lane in D. *, unidentified band. Arrowheads in C and D indicate 90-, 95- and 137-kDa proteins.

was present in the lysate. rCLCA protein was then immunoprecipitated from the cell lysate using the anti-rCLCA antibody bound to rProtein A sepharose. Immunoreactivity of the 86-kDa protein was confirmed by the Western blotting using the same antibody. Streptavidin–HRP recognized the immunoprecipitated 86-kDa protein

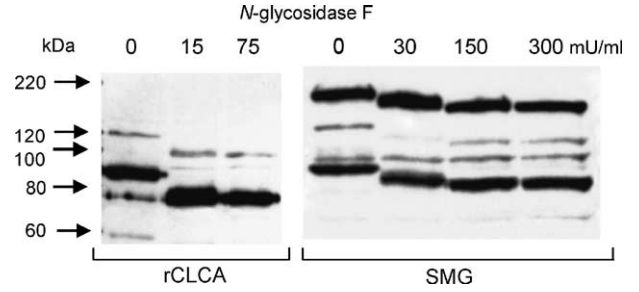

Fig. 6. Digestion by N-glycosidase F of rCLCA-immunoreactive glycoprotein solubilized from membrane fraction of rCLCA-transfected HEK293 cells and rat SMG. Glycosidase digestion was performed prior to reducing SDS-PAGE and Western blotting. Protein loading was 5 μg per rCLCA and 20 μg per SMG lane.

(Fig. 4B), suggesting that the 86-kDa protein should, at least in part, locate on the plasma membrane.

We also confirmed the expression of the rCLCA protein on the plasma membrane by immunocytochemistry, using HEK293 cells transfected with mock or rCLCA vector. The antibody we employed was designed to recognize near the amino-terminus of the molecule. The cell membranes were not pretreated with permealizing agents to enable us to examine whether the epitope site for the antibody exists outside the plasma membrane. The antibody stained the rCLCA-transfected cells, but not the mock-transfected ones (Fig. 5A). Thus, the amino-terminus of rCLCA protein is likely to be located outside the plasma membrane of the transfected cells.

To examine the glycoform pattern of the rCLCA proteins expressed heterologously in HEK293 cells, the membrane fraction was treated with several glycosidases (alone or in combination). N-glycosidase F (15–75 mUnit/ml) reduced the size of the proteins from 120 and 86 kDa to 97 and 75 kDa, respectively (Fig. 6). The sizes of the deglycosylated rCLCA proteins were

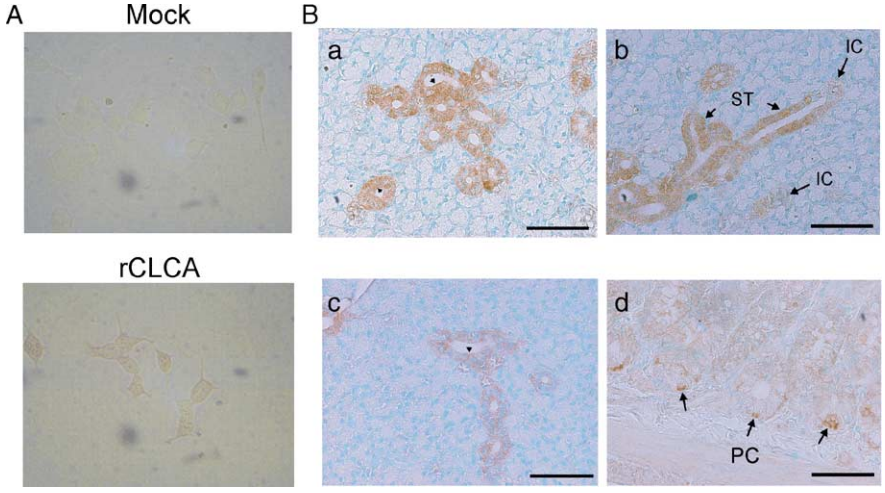

Fig. 5. Immunostaining using anti-rCLCA antibody in non-permealized HEK293 cells transfected with mock or rCLCA vector (A), and in rat submandibular gland (Ba and Bb), parotid gland (Bc), and ileum (Bd). Immunoreactivity at the apical plasma membrane of SMG and PG ducts is indicated by arrowheads. Bar, 50 μm. ST, striated ducts; IC, intercalated ducts; PC, Paneth cells.

consistent with the theoretical molecular weights of 97.9 and 75.9 kDa, respectively, that were calculated from the predicted amino acid sequences (excluding the cleavable amino-terminal signal peptide). In contrast, sialidase (80 mUnit/ml) and O-glycosidase (120 mUnit/ml), either separately or in combination, failed to migrate these bands (data not shown). This result suggests that both protein species are N-linked glycosylated forms.

3.4. Biochemical characterization of salivary rCLCA protein

Rat native tissues were fractionated and analysed by Western blot using the anti-rCLCA antibody (Fig. 4C). The antibody strongly recognized a 95-kDa-sized band in 1 kG Sup, which was prepared from rat SMG lysate under disulfide-reducing conditions. A doublet of bands within the range 90–95 kDa was observed in the membrane fraction. Occasionally, a faint band of 137 kDa was also detected in these fractions (see Figs. 4D and 6A). Notably, an intensely immunoreactive band was found both in 1 kG Sup and in the membrane fraction from SMG at a much higher molecular weight (190 kDa) than those detected in transfected HEK293 cells (which were of 120 and 86 kDa). In contrast, no immunoreactivity at any of above positions was detected in the SMG cytosol in the present study. Any 90-kDa-sized band was below the detection limit in the 1 kG Sup (25 μg protein) from rat ileum and lung (data not shown). Use of 50 μg protein per lane unmasked bands of 90 and 137 kDa in both ileum and lung, whilst the 190-kDa-sized band was never detected in these tissues (Fig. 4D).

Next, to compare the glycoform of the native protein expressed in SMG with that of heterologously expressed rCLCA proteins, we tested the effects of several glycosidases, separately or in combination (Fig. 6). N-glycosidase F (30–300 mUnits/ml) reduced the size of the 190-, 137-, and 90-kDa proteins to 164-, 110-, and 82-kDa, respectively. The latter two bands migrated toward the two bands of the deglycosylated rCLCA protein observed in the transfected cells, although the molecular sizes did not match perfectly. In contrast, sialidase (80 mUnit/ml) and O-glycosidase (60 and 120 mUnit/ml), separately or in combination, failed to shift these bands (data not shown). The 95-kDa protein band appears to be unglycosylated, to judge from the limited migration induced by N-glycosidase F, O-glycosidase, and sialidase. These results suggest that 190-, 137-, and 90-kDa species are linked to N-glycan.

To examine the nature of the 190-kDa protein, solubilized membrane protein was extracted from SDS-acrylamide gel at a position around 190 kDa, and mixed with different concentrations of reducing agent (1, 10, or 500 mM DTT, and 100 or 500 mM β-mercaptoethanol), then heated at 95 °C for 5 min before a second SDS-PAGE. Exposure of the samples to DTT or β-mercaptoethanol at any concentration had no noteworthy effect on the 190-kDa-sized band (data not shown). Thus, the 190-kDa protein is unlikely to be a mutimeric protein complex connected by disulfide bonds in native SMG tissue.

3.5. Immunohistochemical analysis of salivary and ileal rCLCA proteins

Immunohistochemical analysis revealed that intense staining in the ductal epithelia of SMG and PG. The immunoreactivity exhibited both an intracellular and an apical plasma membranous distribution (Fig. 5Ba and 5Bc, arrowheads). The antibody stained the striated ducts intensely, but far less so the intercalated ducts (Fig. 5Bb), while acinar cells were not labeled. In the rat ileum, less intense staining was detected in some of the epithelial cells at the base of the crypts of Lieberkühn (Fig. 5Bd). Those cells were epithelial granulocytes thought to be Paneth cells. The staining pattern was predominantly intracellular, although to the lesser degree there was a basilar membranous distribution. Goblet cells and absorptive surface epithelial cells were negative.

3.6. Functional expression of rCLCA1 in HEK293 cells

We transiently expressed rCLCA1 in HEK293 cells to examine whether the protein can increase Cl^- conductance. The membrane current was measured from hrGFP-positive cells. Fig. 7 shows the effect of a Ca^{2+} ionophore, ionomycin (2 μM), on mock- and rCLCA1-transfected cells. Before perfusion with ionomycin, the basal current density in mock-transfected cells was 2.35 ± 0.28 pA/pF ($n=8$) at 70 mV and -1.31 ± 0.31 pA/pF ($n=8$) at -70 mV. Ionomycin did not alter the current density at either potential, the difference currents being -0.59 ± 0.23 pA/pF at 70 mV and -0.03 ± 0.29 pA/pF at -70 mV ($n=8$).

Among hrGFP-positive cells that had been transfected with rCLCA1, approximately 60% of cells exhibited an apparent increase in conductance in response to ionomycin. The criteria used for the conductance being ionomycin-sensitive were: (i) the outwardly-rectifying current during repetitive voltage ramps developing gradually in the presence of ionomycin, and (ii) the currents being inhibited when Ca^{2+}-free solution, niflumic acid, or DIDS was applied at the end of the experiment. In those transfected hrGFP-positive cells: (a) the basal current density was not different from that obtained in the mock-transfected cells (2.88 ± 0.64 pA/pF at 70 mV, $P=0.59$; -1.67 ± 0.58 pA/pF at -70 mV, $P=0.68$; $n=17$), but (b) the increase in mean current density induced by ionomycin was significantly greater than that observed in mock-transfected cells (7.08 ± 1.01 pA/pF at 70 mV, $P=0.00005$; -4.76 ± 1.17 pA/pF at -70 mV, $P=0.017$; $n=17$). The $I-V$ relationship displayed outward rectification and reversed near 0 mV. In about two thirds of the forty-six rCLCA1-transfected cells examined, depola-

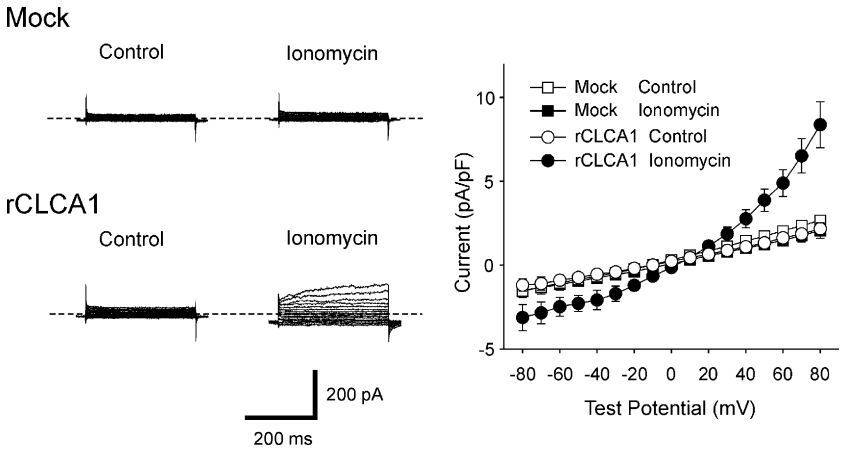

Fig. 7. Functional expression of membrane currents in HEK293 cells transfected with rCLCA1. Ionomycin (2 μM) was used to activate Ca^{2+}-activated Cl^- conductance. (Left) Typical traces recorded from mock- or rCLCA1-transfected cells. Voltage steps (300 ms) were applied from a holding potential of − 50 mV to potentials within the range −80 mV to 80 mV (interval, 10 mV). Broken line denotes basal current at −50 mV. (Right) $I-V$ relationships derived from grouped membrane–current data recorded during voltage steps in the presence or absence of ionomycin in mock-transfected ($n=7$) or rCLCA1-transfected ($n=8$) cells.

rizing and hyperpolarizing pulses induced time-independent currents (see Fig. 8). In the remaining sixteen cells, we observed a slow activation upon depolarization to >50 mV, and deactivation upon hyperpolarization (see Fig. 7). The outward currents evoked by pulses to 80 mV consisted of an instantaneous component followed by a mono-exponential component with a mean time constant of 67.0±17.0 ms (range, 15.4–246.6 ms; $n=13$).

To examine Cl^- dependency, external [Cl^-] was reduced by replacement of NaCl with Na-aspartate ([Cl^-]=11 mM and [aspartate]=140 mM). The intracellular [Cl^-] was 151 mM. The reversal potential of the ionomycin-induced current was 1.0±1.3 mV ($n=6$) in an external [Cl^-] of 151 mM, but 59.8±9.2 mV ($n=5$) in 11 mM [Cl^-], the Cl^- equilibrium potential estimated using the Nernst equation being 0 mV in the former

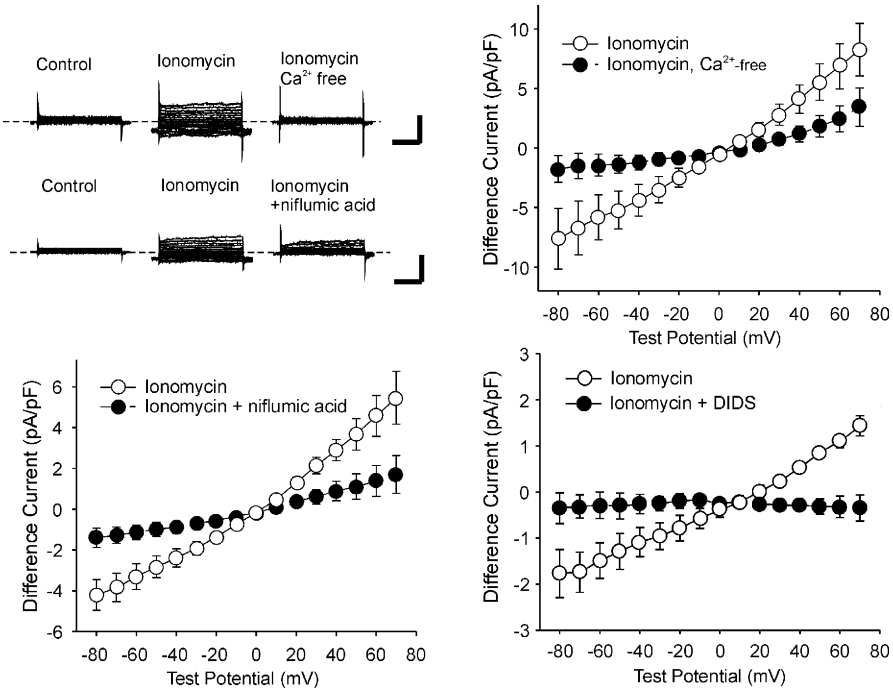

Fig. 8. Typical current traces and $I-V$ relationships obtained from rCLCA1-transfected cells. (Upper left) ionomycin (2 μM) was used to activate Ca^{2+}-activated Cl^- conductance. Treatment with Ca^{2+}-free solution or niflumic acid (100 μM) suppressed the conductance. Voltage steps were applied from a holding current of −50 mV to potentials within the range −80 mV to 80 mV (interval, 10 mV). Broken line denotes basal current at −50 mV. Scales, 100 pA and 100 ms for the upper; 200 pA and 100 ms for the lower. $I-V$ relationships were derived from grouped membrane–current data before and during treatment with Ca^{2+}-free solution ($n=6$), niflumic acid (100 μM, $n=6$), and DIDS (100 μM, $n=4$). Difference current at each step potential was obtained by subtracting current recorded before adding ionomycin from that recorded during treatment (ionomycin plus either Ca^{2+}-free solution or one of the above agents).

external [Cl^-], and 66.5 mV in the latter. This suggests that the current was entirely [Cl^-]-dependent. The difference between the experimentally obtained reversal potential and the Cl^- equilibrium potential indicates a slight aspartate permeability through the channel. To exclude the possibility of an involvement of cation conductance, the reversal potential was measured in an external solution in which Na^+ had been replaced by *N*-methyl-D-glucamine (NMDG). The switch from Na^+ to NMDG did not alter the reversal potential of the current evoked by ionomycin (-0.2 ± 2.8 mV, $n=4$).

We tested the channel's requirement for external Ca^{2+} and its sensitivity to compounds affecting anion permeability. Perfusion with an external solution not containing Ca^{2+} reduced the ionomycin-induced current (Fig. 8). The difference current density was significantly decreased from 6.86 ± 1.89 to 2.45 ± 1.09 pA/pF at +60 mV ($P=0.031$, $n=6$) and from -5.82 ± 1.89 to -1.43 ± 0.92 pA/pF at −60 mV ($P=0.018$, $n=6$) (Fig. 8). Niflumic acid (100 μM), known to be a potent inhibitor of Ca^{2+}-activated Cl^- channels, decreased the effect of ionomycin, too (Fig. 8), the difference current density being reduced from 4.57 ± 1.00 to 1.38 ± 0.75 pA/pF at 60 mV ($P=0.0014$, $n=6$) and from -3.31 ± 0.63 to -1.14 ± 0.36 pA/pF at −60 mV ($P=0.0014$, $n=6$). DIDS (100 μM), a stilbene compound, also inhibited the channel activity (Fig. 8). At positive potentials, the currents were reduced to beneath the control current level, indicating that a portion of the basal current was DIDS-sensitive. The difference current density was decreased from 1.11 ± 0.14 to -0.32 ± 0.23 pA/pF at 60 mV ($P=0.014$, $n=4$) and from -1.49 ± 0.39 to -0.29 ± 0.29 pA/pF at −60 mV ($P=0.033$, $n=4$).

4. Discussion

Alignment of the deduced amino acid sequences for members of the CLCA family shows that the predicted amino acid sequence for rCLCA1 is closely related to those of the mouse homologues mCLCA1, 2, and 4. Several consensus motifs that may be functionally important are well preserved among CLCA members [7–16,21]. The existence of the amino-terminal signal sequence in rCLCA1 indicates that the amino-terminus is located extracellularly. This was confirmed by the specific immunocytostaining detected on the plasma membrane of HEK293 cells transfected with rCLCA1 using an antibody raised against the region near the amino-terminus. A consensus proteolytic cleavage site was found at residue S701. The prediction of two cleavage products is supported by the present immunoblotting analysis revealing the existence of two protein species for the rCLCA1-transfected HEK293 cells. It is likely that the translational product of 120 kDa, which was detected as a faint band, is cleaved into at least two parts, one of which is intensively labeled as an 86 kDa component. This result is consistent with the reported posttranslational cleavage of CLCA members [8].

The present electrophysiological results show that expression of rCLCA1 in HEK293 cells creates a Ca^{2+}-activated Cl^- conductance. A Ca^{2+} ionophore, ionomycin, elicited an outwardly rectifying current in these rCLCA1-transfected cells, but not in non-transfected or mock-transfected cells. The rCLCA1-associated currents were sensitive to niflumic acid and DIDS, which have been used to inhibit endogenous Ca^{2+}-activated Cl^- channels [2]. Further, the reversal potential of the rCLCA1-induced current was shifted by a change in the [Cl^-] gradient between the inside and outside of the cells. These features are consistent with those reported for other CLCA members [10,11,14], with some exceptions in the case of the pharmacological characteristics of the bovine isoform (e.g., no effects of niflumic acid on bCLCA1 or DIDS on pCLCA1) [7,22].

In native cells, the whole-cell currents induced either by ionomycin plus external Ca^{2+} or by intracellular Ca^{2+} in the patch pipette exhibit voltage-dependent features distinct from those of the Cl^- currents mediated by known CLCA members [23]. A native cell-specific feature is that depolarization evokes a slowly developing current, while repolarization causes a decaying current. The rCLCA1-mediated current recorded from some of our cells had a characteristic similar to that mentioned above for native cells. According to recent reports, pCLCA1-associated Cl^- currents exhibit a similar characteristic [22] and its expression may increase the sensitivity of preexisting endogenous Cl^- channels [24]. In the case of native Cl^- channels, it has been shown that the time-dependency of the current during voltage steps and the rectification displayed by the $I-V$ curve are correlated with a voltage-dependent sensitivity of the channels to intracellular [Ca^{2+}] [25,26]. Thus, the variability of the time-dependency observed in the present study is likely to reflect sensitivity of endogenous Cl^- channels to different increases in the intracellular [Ca^{2+}] by ionomycin.

Western blotting analysis demonstrated that the present anti-rCLCA antibody reacts with several bands of 137- and 90-kDa proteins obtained from rat SMG, ileum, and lung. The absence of detectable labeling in the cytosolic fraction indicates that the proteins mainly associate with the plasma membrane and intracellular membranes, and that they are unlikely to be cytosolic proteins. The 95-kDa protein band appears to be unglycosylated because of the limited migration induced by N-glycosidase F, O-glycosidase, or sialidase. In contrast, the 137- and 90-kDa proteins are likely to be N-linked glycoforms since digestion with N-glycosidase F markedly reduced their apparent molecular sizes (to 110 and 82 kDa, respectively). Thus, these glycoproteins are likely to be processed in the same manner as recombinant proteins in rCLCA-transfected HEK293 cells, in which 97- and 75-kDa proteins were glycosylated to produce 120- and 86-kDa forms, respectively.

Interestingly, a 190-kDa N-linked glycoprotein was detected in SMG, but not in either ileum or lung. This band is unlikely to represent a disulfide-bound mutimeric protein complex since treatment with SDS under highly reducing conditions failed to migrate the band. We cannot rule out the possibility of non-specific binding of the present antibody to a SMG-specific protein. Thus, the mammalian protein database was scanned using the BLAST algorism, and no protein other than CLCA members was found to possess an amino acid homology to the epitope for the present antibody. Further biochemical experiment is required to investigate the molecular nature and functional significance of the 190-kDa rCLCA-like protein found in SMG.

Both the mRNA and the protein for rCLCA1 were found to be expressed in SMG, ileum, and lung. At the level of mRNA expression, mCLCA1 has been reported to be present in ileum, lung, liver, and spleen [21], a localization pattern similar to that detected here for rCLCA1. On the other hand, hCLCA1 and hCLCA4 are expressed in intestine, but not in lung [9,10], while hCLCA2 is expressed in the trachea, but not in intestine or kidney [11]. The mCLCA6 mRNA has been found to be expressed in intestine, although it was undetectable in lung [13]. The present immunohistochemical results revealed a pattern of localization for rCLCA1 protein distinct from those reported for the murine CLCA members. Here, an expression of rCLCA1 was found in SMG ducts, but not in the acini, whereas mCLCA1 mRNA has been reported to be located in salivary acini on the basis of an in situ hybridization study [21]. Rat CLCA1 was mainly expressed in cells presumed to be Paneth cells at the base of the ileal crypts, but not in other crypt cells (epithelial, goblet, or villous cells). Murine CLCA1 is reportedly present predominantly in the crypt, and either weakly or not at all in the villi, of ileum and colon [21]. In contrast, mCLCA3 has been found predominantly in goblet cells [27], while mCLCA4 is in the villi, but not in crypt or goblet cells [12], and hCLCA1 is in the basal crypt and goblet cells of the intestine [10]. Taking all this together, rCLCA1 appears to exhibit a strikingly distinctive expression pattern of tissue localization. The presence of dense intracellular immunostaining in the above tissues raises questions about the subcellular localization of rCLCA protein (e.g., its possible localization in intracellular organellae and/or vesicles involved in membrane trafficking along secretory and endocytic pathways).

Only recently, Jeong et al. reported a new homolog (rbCLCA) cloned from the rat brain [28]. The amino acid sequence of rCLCA1 differs from that of rbCLCA especially in the C-terminal region, which was shown to be close to that of mCLCA4. The expression of rbCLCA mRNA also appears to be distinct from that of rCLCA1, being predominantly in neural tissues, the kidney and small intestine but not in the liver, lung or spleen [28]. Because of the similarity of the amino acid sequences, the epitope used for the anti-rCLCA antibody exists in rbCLCA as well. Thus, the tissue expression patterns of these isoforms need to be compared precisely. Differences in the electrophysiological profiles of these isoforms were also observed: rbCLCA possessed a slight rectification of the $I-V$ relationship and a time-dependent decay of the currents [28]. However, it should be noted that the rbCLCA mRNA sequence cannot be aligned appropriately in a manner that corresponds to the rat genome sequence [19] according to a BLAST search using the contig NW_047633 residing in rat chromosome 2. In fact, the rbCLCA mRNA was found to separate into two distinct genes that have been predicted by computational analysis based on the rat genome (XM_342354 for ca. 230 nucleotides in the 3′-terminal region of rbCLCA and XM_575054 for the rest). In contrast, the full sequence of rCLCA1 mRNA corresponds entirely to the genome sequence (14 exons). This contradiction needs to be fully resolved to make meaningful physiological and immunohistological comparisons between these rat isoforms.

The expression of rCLCA1 in epithelial cells made it likely that it is involved in modulation of transepithelial Ca^{2+}-dependent secretion or reabsorption of Cl^-. The present study demonstrated the specific existence of rCLCA1 in striated ductal cells in which the epithelium is known to reabsorb much of the NaCl that is secreted from acinar cells isotonically, thus making the final saliva hypotonic [6]. Several types of Cl^- channels, including CFTR and Ca^{2+}-activated Cl^- channels, have been found in rat SMG duct cells [29,30]. The mechanism is still debatable, as it is for unidirectional Cl^- transport in the ductal epithelium of salivary glands [6]. A "push–pull" mechanism of unidirectional Cl^- transport has been proposed for the pancreas by which cholinergic stimulation causes cytosolic Ca^{2+} gradients, and in turn a heterogeneous activation of Ca^{2+}-activated Cl^- channels that triggers unidirectional Cl^- transport [31]. Rat CLCA1 may play a certain role in Cl^- influx through the apical membrane [which is initially enhanced by depolarization driven by activation of epithelial Na^+ channels (ENaC)], followed by Cl^- efflux through the basolateral membrane.

In conclusion, we have identified a rat CLCA homologue expressed in salivary duct cells. The specific distribution of rCLCA1 in the duct cells suggests a modulatory role in the unidirectional transport of Cl^-. A functional consequence of cystic fibrosis is a defect in Cl^- transport in the ductal cells of the salivary glands and pancreas [29]. Further investigation is needed to establish whether rCLCA1 protein might be able to compensate for the loss of ductal function in cystic fibrosis. In addition to the monobasic proteolysis and N-glycosylation commonly observed in heterologous expression systems and native tissues, we found a SMG-specific high molecular mass protein immunoreactive to the anti-rCLCA antibody. It will be an important future project to investigate the functional significance of such different protein species expressed in salivary glands.

Acknowledgements

We thank Dr. R. Timms for editing the English. This work was supported by a grant-in-aid from the Ministry of Education, Science, Sports and Culture of Japan (Frontier Research Grant) and by a grant from Suzuken Memorial Foundation.

References

[1] J.R. Hume, D. Duan, M.L. Collier, J. Yamazaki, B. Horowitz, Anion transport in heart, Physiol. Rev. 80 (2000) 31–81.
[2] T.J. Jentsch, V. Stein, F. Weinreich, A.A. Zdebik, Molecular structure and physiological function of chloride channels, Physiol. Rev. 82 (2002) 503–568.
[3] J. Yamazaki, J.R. Hume, Inhibitory effects of glibenclamide on cystic fibrosis transmembrane regulator, swelling-activated and Ca^{2+}-activated Cl^- channels in mammalian cardiac myocytes, Circ. Res. 81 (1997) 101–109.
[4] J. Yamazaki, K. Kitamura, Cell-to-cell communication via nitric oxide modulation of oscillatory Cl^- currents in rat intact cerebral arterioles, J. Physiol. (Lond.) 536 (2001) 67–78.
[5] C.M. Fuller, D.J. Benos, Electrophysiological characteristics of the Ca^{2+}-activated Cl^- channel family of anion transport proteins, Clin. Exp. Pharmacol. Physiol. 27 (2000) 906–910.
[6] J.E. Melvin, Chloride channels and salivary gland function, Crit. Rev. Oral Biol. Med. 10 (1999) 199–209.
[7] S.A. Cunningham, M.S. Awayda, J.K. Bubien, I.I. Ismailov, M. Pia Arrate, B.K. Berdiev, D.J. Benos, C.M. Fuller, Cloning of an epithelial chloride channel from bovine trachea, J. Biol. Chem. 270 (1995) 31016–31026.
[8] R.C. Elble, J. Widom, A.D. Gruber, M. Abdel-Ghany, R. Levine, A. Goodwin, H.-C. Cheng, B.U. Pauli, Cloning and characterization of lung-endothelial cell adhesion molecule-1 suggest it is an endothelial chloride channel, J. Biol. Chem. 272 (1997) 27853–27861.
[9] M. Agnel, T. Vermat, J.-M. Culouscou, Identification of three novel members of the calcium-dependent chloride channel (CaCC) family predominantly expressed in the digestive tract and trachea, FEBS Lett. 455 (1999) 295–301.
[10] A.D. Gruber, R.C. Elble, H.-L. Ji, K.D. Schreur, C.M. Fuller, B.U. Pauli, Genomic cloning, molecular characterization, and functional analysis of human CLCA1, the first human member of the family of Ca^{2+}-activated Cl^- channel proteins, Genomics 54 (1998) 200–214.
[11] A.D. Gruber, K.D. Schreur, H.-L. Ji, C.M. Fuller, B.U. Pauli, Molecular cloning and transmembrane structure of hCLCA2 from human lung, trachea, and mammary gland, Am. J. Physiol., Cell Physiol. 276 (1999) C1261–C1270.
[12] R.C. Elble, G. Ji, K. Nehrke, J. DeBiasio, P.D. Kingsley, M.I. Kotlikoff, B.U. Pauli, Molecular and functional characterization of a murine calcium-activated chloride channel expressed in smooth muscle, J. Biol. Chem. 277 (2002) 18586–18591.
[13] S.R. Evans, W.B. Thoreson, C.L. Beck, Molecular and functional analyses of two new calcium-activated chloride channel family members from mouse eye and intestine, J. Biol. Chem. 279 (2004) 41792–41800.
[14] R. Gandhi, R.C. Elble, A.D. Gruber, K.D. Schreur, H.-L. Ji, C.M. Fuller, B.U. Pauli, Molecular and functional characterization of a calcium-sensitive chloride channel from mouse lung, J. Biol. Chem. 273 (1998) 32096–32101.
[15] D. Lee, S. Ha, Y. Kho, J. Kim, K. Cho, M. Baik, Y. Choi, Induction of mouse Ca^{2+}-sensitive chloride channel 2 gene during involution of mammary gland, Biochem. Biophys. Res. Commun. 264 (1999) 933–937.
[16] K.J. Gaspar, K.J. Racette, J.R. Gordon, M.E. Loewen, G.W. Forsyth, Cloning a chloride conductance mediator from the apical membrane of porcine ileal enterocytes, Physiol. Genetics 3 (2000) 101–111.
[17] B.U. Pauli, M. Abdel-Ghany, H.-C. Cheng, A.D. Gruber, H.A. Archibald, R.C. Elble, Molecular characteristics and functional diversity of CLCA family members, Clin. Exp. Pharmacol. Physiol. 27 (2000) 901–905.
[18] Z. Qu, R.W. Wei, W. Mann, H.C. Hartzell, Two bestrophins cloned from *Xenopus laevis* oocytes express Ca^{2+}-activated Cl^- currents, J. Biol. Chem. 278 (2003) 49563–49572.
[19] Rat Genome Sequencing Project Consortium, Genome sequence of the Brown Norway rat yields insights into mammalian evolution, Nature 428 (2004) 493–521.
[20] S.F. Altschul, T.L. Madden, A.A. Schaffer, J. Zhang, Z. Zhang, W. Miller, D.J. Lipman, Gapped BLAST and PSI-BLAST: a new generation of protein database search programs, Nucleic Acids Res. 25 (1997) 3389–3402.
[21] A.D. Gruber, R. Gandhi, B.U. Pauli, The murine calcium-sensitive chloride channel (mCaCC) is widely expressed in secretory epithelia and in other select tissues, Histochem. Cell. Biol. 110 (1998) 43–49.
[22] M.E. Loewen, S.E. Gabriel, G.W. Forsyth, The calcium-dependent chloride conductance mediator pCLCA1, Am. J. Physiol., Cell Physiol. 283 (2002) C412–C421.
[23] F.C. Britton, S. Ohya, B. Horowitz, I.A. Greenwood, Comparison of the properties of CLCA1 generated currents and $I_{Cl(Ca)}$ in murine portal vein smooth muscle cells, J. Physiol. (Lond.) 539 (2002) 107–117.
[24] M.E. Loewen, L.K. Bekar, W. Walz, G.W. Forsyth, S.E. Gabriel, pCLCA1 lacks inherent chloride channel activity in an epithelial colon carcinoma cell line, Am. J. Physiol.: Gastrointest. Liver Physiol. 287 (2004) G33–G41.
[25] J. Arreola, J.E. Melvin, T. Begenisich, Activation of calcium-dependent chloride channels in rat parotid acinar cells, J. Gen. Physiol. 108 (1996) 35–47.
[26] A. Kuruma, H.C. Hartzell, Bimodal control of a Ca^{2+}-activated Cl^- channel by different Ca^{2+} signals, J. Gen. Physiol. 115 (2000) 59–80.
[27] I. Leverkoehne, A.D. Gruber, The murine mCLCA3 (alias gob-5) protein is located in the mucin granule membranes of intestinal, respiratory, and uterine goblet cells, J. Histochem. Cytochem. 50 (2002) 829–838.
[28] S.M. Jeong, H.-K. Park, I.-S. Yoon, J.-H. Lee, J.-H. Kim, C.-G. Jang, C.J. Lee, S.-Y. Nah, Cloning and expression of Ca^{2+}-activated chloride channel from rat brain, Biochem. Biophys. Res. Commun. 334 (2005) 569–576.
[29] A.E.O. Trezise, M. Buchwald, In vivo cell-specific expression of the cystic fibrosis transmembrane conductance regulator, Nature 353 (1991) 434–437.
[30] W. Zeng, M.G. Lee, S. Muallem, Membrane-specific regulation of Cl^- channels by purinergic receptors in rat submandibular gland acinar and duct cells, J. Biol. Chem. 272 (1997) 32956–32965.
[31] H. Kasai, G.J. Augustine, Cytosolic Ca^{2+} gradients triggering unidirectional fluid secretion from exocrine pancreas, Nature 348 (1990) 735–738.